iJRASET
International Journal For Research in Applied Science and Engineering Technology

INTERNATIONAL JOURNAL FOR RESEARCH

IN APPLIED SCIENCE & ENGINEERING TECHNOLOGY

Volume: 5 **Issue:** XI **Month of publication:** November 2017

DOI: http://doi.org/10.22214/ijraset.2017.11106

www.ijraset.com

Call: 08813907089 | E-mail ID: ijraset@gmail.com

International Journal for Research in Applied Science & Engineering Technology (IJRASET)
ISSN: 2321-9653; IC Value: 45.98; SJ Impact Factor:6.887
Volume 5 Issue X1, November 2017- Available at www.ijraset.com

Reduction of Organic Dye Using Anatase Tio_2 Nanocrystallites under Solar-Irradiation: Effect of Particle Size

S. Sharmila Juliet[1], S. Ramalingom[2], C. Ravidhas[3], A. Moses Ezhil Raj[4]
[1, 4] *Department of Physics & Research Centre, Scott Christian College (Autonomous), Nagercoil-629003, India.*
[2] *Department of Physics, Vivekananda College, Agasteeswaram-629701, India.*
[3] *Departments of Physics, Bishop Heber College (Autonomous), Thiruchirapalli-620 017, India.*

Abstract: ***Anatase titanium oxide (TiO_2) nanocrystallites with tetragonal structure (4/mmm) and space group $I4_1/amd–D_{4h}^{19}$ were synthesized via sol-gel route, followed by calcination at two different temperatures 400 and 600 °C, to study the effect on photocatalytic reduction of methyl orange (MO) dye. Structural parameters and its variation with calcination temperature for the prepared samples were analyzed using X-ray diffraction pattern. The metal-oxide phase formation was again confirmed from the band assignments of the Fourier transform infrared spectra. Effect of calcination temperature on particle size of the TiO_2 samples was accurately analyzed directly from transmission electron micrographs. Elemental analysis has been performed to identify the purity of the prepared samples. The optical parameters were extracted from the optical absorption data, the band gap values of the TiO_2 powder sample varies from 3.24 to 3.06 eV as calcination temperature increases. The photocatalytic activities of the products were evaluated by studying the degradation of MO dye in aqueous solution by direct solar irradiation. The anatase TiO_2 calcined at 400 ^oC shows 100 % degradation of MO because of its smaller particle size (9.8 nm) exactly at 3.5 h. Based on the obtained results, the particle size of TiO_2 powders has pronounced influence in photocatalytic activity.***
Keywords: Nano structures, Titanium oxide, Sol-gel, X-ray diffraction, Optical bandgap, Photocatalyst.

I. INTRODUCTION

Synthetic dyes comprise an important part of industrial water effluents, as they are discharged in abundance by many manufacturing industries. The impact of these dyes on the environment is a major concern because of the potentially carcinogenic properties of these chemicals [1]. Some azo dyes may be able to cause mutations and be associated with the development of bladder cancer. Besides this, some dyes can undergo anaerobic decolouration to form potential carcinogens [2, 3]. The wastewater which is colored in the presence of these dyes can block both sunlight penetration and oxygen dissolution, which are essential for aquatic life. Among them, MO is an intensely colored compound used in dyeing and printing textiles as a dyestuff. Thus there is a considerable need to treat these colored effluents before discharging them to various water bodies. Various physicochemical techniques are available for the elimination of dyes from wastewater and in particular photocatalysis is a more promising cost effective tool. Moreover, photocatalysis can be used to cause redox transformations and decompose a dye molecule. The use of photosensitive semiconductors such as TiO_2, ZnO, Fe_2O_3, CdS, ZnS and V_2O_5 has been reported in the literature for their use in reducing color of the dye solutions owing to their environmental friendly benefits in the saving of resources such as water, energy, chemicals and other cleaning materials [4-8]. Methylene blue, Crystal violet, Congo-red, Phenol like organic dye molecules were already degraded by using TiO_2 nanoparticles as reported [9-11].

Titanium dioxide (TiO_2) mediated based photodegradation has attracted extensive interest owing to its great advantages in the complete removal of organic pollutants from wastewater [12]. This is mainly because of its various merits, such as optoelectronic properties, low-cost, chemical stability and non toxicity [13]. Excitation with light on TiO_2 produce pairs of holes (h^+) and electrons (e^-), which can either recombine inside or on the surface of titania or react with adsorbed electron donors (e.g. hydroxide ions) or acceptors (e.g. oxygen). The resulting hydroxyl radicals $OH^•$ and superoxide ions $O_2^{-•}$ are known to be oxidants capable of oxidizing organic compounds [14].

For such applications, TiO_2 exhibiting its anatase phase have been prepared using different methods such as, DC magnetron sputtering [15], hydrothermal [16, 17], solvo thermal method [18], emulsion precipitation and sol–gel method [19, 20]. Among the various methods available, sol–gel route has been regarded as an excellent method to synthesize nano-sized metallic oxides [21, 22] and has been widely employed for the preparation of titanium dioxide nano-particles [23, 24]. Because of synthesis from atomic or

molecular precursors, sol–gel technique can give better control of particle size and homogeneity in particle distribution [25, 26]. Keeping the above aspects, we report in this paper the synthesis of fine nanostructured TiO_2 photocatalyst through cost effective sol-gel technique using titanium tetra-isopropoxide as a precursor material and its particle size dependent photodegradation of MO.

II. EXPERIMENTAL PROCEDURE

A. Powder synthesis

The pure TiO_2 nanocrystalline powders have been prepared using 8 ml of Titanium tetra-isopropoxide [$Ti(OiPr)_4$] as the starting precursor and were then dissolved in 50 ml ethanol under constant magnetic stirring [24]. The sol obtained after 45 min was then converted into gel by adding 100 ml of de-ionized water. The suspension obtained was left at room temperature for 15 min and then filtered to obtain a white precipitate. The precipitate was washed with both distilled water and ethanol followed by centrifugation to remove impurities. Three main reactions that occur during the sol-gel process are hydrolysis, alcohol condensation and water condensation. The reaction is as follows [27];

$Ti - OR + H_2O \rightarrow Ti - OH + R - OH$ Hydrolysis

$Ti - OH + RO - Ti \rightarrow Ti - O - Ti + R - OH$ Alcohol condensation

$Ti - OH + HO - Ti \rightarrow Ti - O - Ti + H_2O$ Water condensation

Finally, the powders were dried in air at 100 ºC for 1h and then calcined at 400 ºC and 600 ºC for 2 h in a muffle furnace with a heating rate of 10 ºC per min.

B. Powder characterization

Structural investigations were performed using X-ray diffraction spectra recorded in the PHILIPS X'pert-Pro diffractometer. Continuous scanning of the sample was done in the θ-2θ mode using a copper target (λ=1.5406 Å) for the step size of 0.03°. FTIR spectrum was recorded in the spectral range of 400-4000 cm^{-1} with a Thermo Nicolet, Avatar 370 spectrometer. Compositions of the synthesized particles were determined by Energy dispersive spectrum (EDS) using a JEOL Model JED - 2300 microscope. The Transmission electron microscopy (TEM) was analyzed using PHILIPS Model CM200. The optical absorption spectra were recorded in the wavelength range 200-2500 nm using Varian Cary 5000 spectrophotometer. The photocatalytic degradation of methyl orange dye aqueous solution was evaluated by under solar irradiation.

III. RESULTS AND DISCUSSION

A. Structural analysis

From the X-ray diffraction spectra as shown in Fig. 1, it is evident that the as-prepared TiO_2 sample is almost amorphous having broad base separation, while the calcined samples are crystalline that shows peaks in respective 2θ positions pertinent to its anatase phase. However, the diffraction peak intensity of all the peaks enhances on calcination at 400 ºC and 600 ºC. On calcination, the width of (101) plane at 2θ=25 º becomes narrow, indicating the improvement of crystallization of anatase phase as already reported [28]. All the peaks were indexed for its anatase phase based on the standard data (JCPDS file no.: 71- 1166). Absence of impurity peaks other than the anatase phase confirms the phase/material purity of the prepared products. Observed anatase phase belongs to the space group $I4_1/amd$ that consist of TiO_6 octahedral sharing with four edges. Broad diffraction lines of TiO_2 nano powder sample calcined at 400 ºC entail small crystallite size.

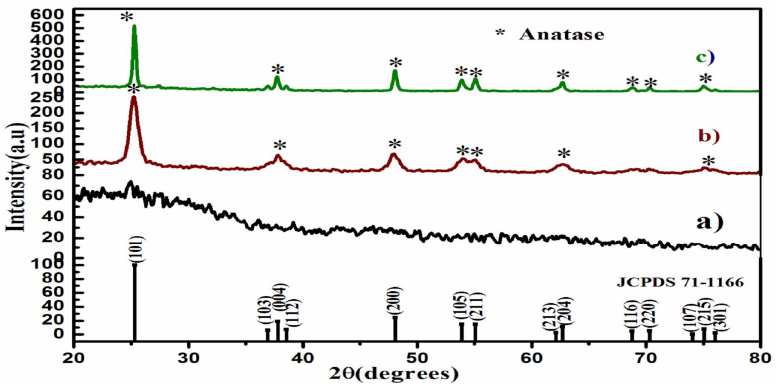

Fig. 1: XRD patterns of sol–gel synthesized titanium oxide nanopowder a) as prepared b) calcined at 400ºC and c) calcined at 600ºC for 2h.

Mean crystallite sizes of calcined powder samples were evaluated using the Scherrer's formula [29]. Estimated crystallite size from the Scherrer's equation was found to increase from 14.66 to 41 nm as the calcination temperature increases from 400 to 600ºC. The crystallite size of the samples was also estimated from the Scherrer's plot. Calcination temperature has a significant role in deciding the crystallite size and crystallinity of the product.

Since TiO_2 anatase has tetragonal lattice, the unit cell edges of the synthesized photocatalyst were calculated for a tetragonal structure where a=b≠c. Calculated lattice parameters of the powder samples TiO_2 calcined at 400 and 600 ^oC respectively are comparable to the JCPDS standards. As the calcination temperature increases from 400 to 600 ^oC, the lattice constant *c* = 9.499 Å slightly increases to 9.518 Å that indicates elongation along the c-axis due to the presence of tensile stress. During calcination, generally lattice defects and stains decreases, it can cause coalescence of the crystallites that result in increasing the average size of the particles. The surface area of the prepared TiO_2 samples has been measured and the sample calcined at 400 ^oC shows the large surface area to volume ratio which increases the surface specific active sites for chemical reactions and photon absorptions. All the calculated lattice parameters are listed in Table.1, and it is evident that the calcination temperature has a profound effect on structural parameters.

Table 1: Structural and optical parameters of synthesized anatase TiO2 nano particles

Sample details	Crystallite size, D (nm)				Lattice parameters		Micro strain $\varepsilon x10^{-4}$	Unit cell volume V ($Å^3$)	Density ρ (g/cm^3)	Surface area S (cm^2/g)	Optical bandgap (eV)
	Scherrer formula	Scherrer plot	W-H plot	TEM	a (Å)	c (Å)					
As-syn	-	-	-		-	-	-		-	-	3.24
TiO_2 400	14.66	16.86	9.81	9.5	3.788	9.499	-15.9	136.34	3.891	157	3.19
TiO_2 600	41.00	42.22	33.21	29	3.787	9.518	-4.32	136.49	3.887	46	3.06
JCPDS					3.784	9.515		136.25	3.895		

The traditional line profile analysis method like Williamson-Hall is useful for a preliminary screening of the data plot [30, 31]. The mean crystallite size of calcined TiO_2 powder and the amount of internal strain created within the samples were determined by this method according to the Williamson-Hall equation [32, 33]. It is observed that the micro strain decreases when crystalline size increases.

B. Vibrational Analysis

The FT-IR spectra of synthesized titanium dioxide powder samples are depicted in the Fig. 2. Formation of TiO_2 phase can be confirmed from the Ti - O stretching vibration in the low energy region (below 800 cm^{-1}). The appearance of the large broad band in the range 500–900 cm^{-1} with maximum absorption at 470 to 515 cm^{-1} is probably the characteristics of Ti–O–Ti anatase structure [34-36]. This band is due to stretching mode of Ti–O (–Ti–O) which was the envelope of the phonon bands of a Ti–O–Ti bond of a titanium oxide network could be assigned

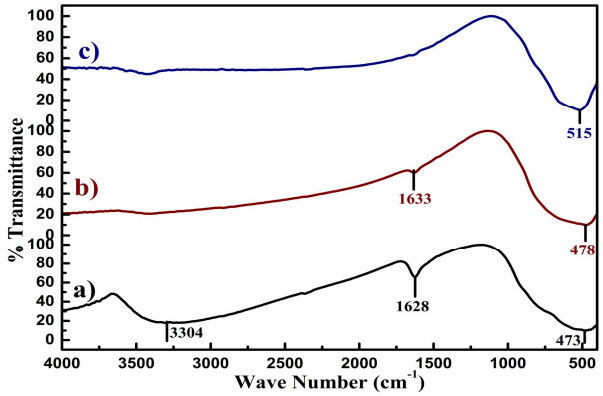

Fig. 2: FT-IR spectra of titanium oxide samples a) as synthesized b) calcined at 400ºC and c) calcined at 600ºC for 2h.

The characteristic absorption peak of (OR) group of titanium isopropoxide, which was the precursor of the sols, is in the range 1085–1050 cm^{-1}[37]. Owing to the fact that no absorption peak was detected in this range is concluded that all four (OR) groups of titanium isopropoxide were substituted with (OH) groups of water. Thus, a full conversion of the precursor is obtained by the hydrolysis reaction, resulting the formation of TiO_2 particles. The absorption peaks approximately at 1630 cm^{-1} in the wave number range 1650–1600 cm^{-1} indicates the incorporation of water in the as-prepared samples. However, these absorption bands are disappeared on heating to 600 °C. The removal of these peaks after calcinations indicates the removal of adsorbed water from the as-prepared sample. Additional broad absorption peak in the range 3370–3097 cm^{-1} is due to the stretching vibration of the hydroxyl (O–H) bond in the un-calcined as prepared sample TiO_2. The low intensity of these peaks in the calcined samples indicates the removal of a large portion of adsorbed water from TiO_2.

C. Elemental Analysis

The electron dispersive spectrum (EDS) results shown in Fig. 3 reveal that all powder samples are containing only the elements Ti and O. No impurity elements could be detected within the detection limits. EDS for the as prepared and calcined TiO_2 powder samples show a peak around 0.5 keV for 74.82% of O atoms and another intense peak appears at 4.5 keV for 25.18% of Ti atoms which confirms the purity of the synthesized samples.

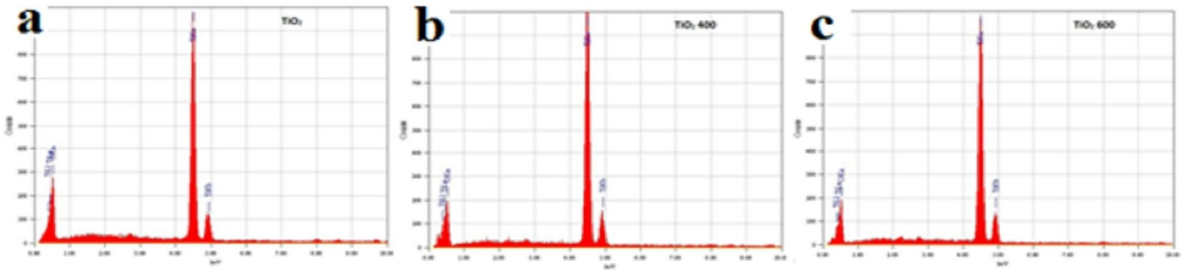

Fig. 3: Edax Analysis Of The (A) As Prepared (B) Titanium Oxide Powders Calcined At 400°c (C) Calcined At 600°c For 2 H.

D. Morphological Analysis

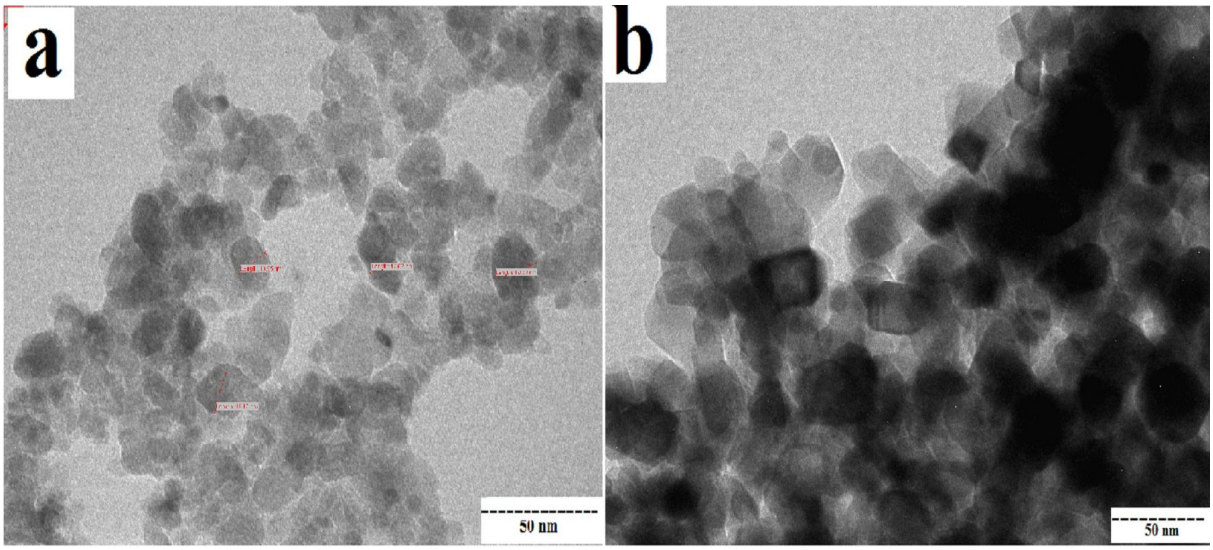

Fig. 4: TEM images and diffraction pattern for the prepared titanium oxide nano powders calcined at (a) 400°C (b) 600°C for 2h.

Transmission electron microscope (TEM) is also used to investigate the crystallinity, shape, and morphology as well as the particle size of the synthesized samples. In this tool, data fetch is direct and less likely to be affected by the experimental errors and other properties of the particles such as internal strain or variation in the size of the lattice parameter. Fig. 4 shows the TEM micrograph of the calcined TiO_2 anatase samples, from which it can be seen that samples TiO_2 calcined at 400 °C and 600 °C has well-defined granules with an average size of 9.5 nm and 29 nm respectively and it is comparable with the XRD results. As can be seen, calcined sample at 400°C are spherical in shape and the size distribution is uniform.

E. Optical characterization

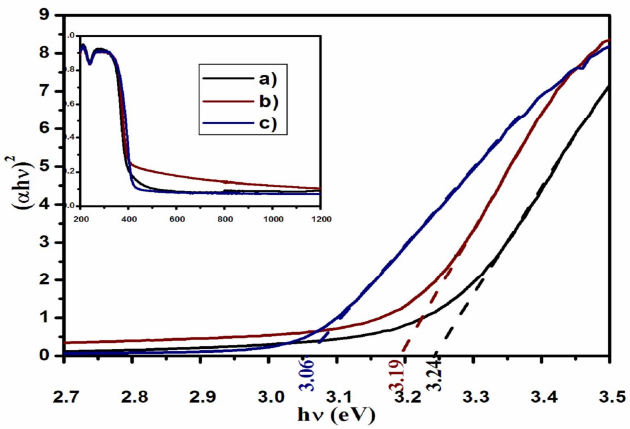

Fig. 5: UV-Absorbance spectra of a) as prepared b) titanium oxide nano samples calcined at 400°C and c) calcined at 600°C for 2h. Inset is the Tauc plot

UV-visible absorption measurement was carried out in order to obtain the optical parameters of the TiO_2 nanopowder. The absorption spectrum of nano TiO_2 (Inset of Fig. 5) consists of a single and broad intense absorption around 400 nm due to charge transfer from the valence band (formed by 2p orbitals of the oxide anion) to the conduction band formed by 3d t_{2g} orbitals of the Ti^{4+} cations [38]. The band gap can be estimated from a plot of $(\alpha h\nu)^2$ vs photon energy ($h\nu$) as seen Fig. 5. The intercept of the tangent to the plot will give a good approximation of the band gap energy for this direct band gap material [39]. It can be seen that all samples were strong absorptions in the ultraviolet region. The absorption edge of annealed TiO_2 samples moved to longer wavelength in comparison with synthesized TiO_2 indicating the band gap was decreased by increasing the calcination temperature. Obtained band gap values of the TiO_2 powder samples are listed in Table.1, which varies from 3.24 to 3.06 eV as calcination temperature increases. Thus the size quantization increases the energy band gap between the conduction band electrons and valence band holes which leads to change in their optical properties.

F. Photocatalytic degradation

Degradation activity was studied under direct sunlight by mixing synthesized TiO_2 ($5x10^{-3}$ M) in water (100 ml) containing $1x10^{-4}$ M of methyl orange dye. When this suspension is irradiated, electrons are excited from the valence to the conduction band, generating positive holes and electrons [40]. These positive holes can react with electron donors in the solution to produce hydroxyl radicals or would directly oxidize organic molecules at the semiconductor surface. The hydroxyl radicals generated in the process are strong oxidants and react quickly with the organic matter adsorbed on the catalyst, forming oxidized intermediates, and if the treatment time is adequate, complete mineralization is achieved. The typical mechanism involving hydroxyl oxidative radical reactions go through the steps: electron transfer, hydrogen abstraction and addition to aromatic rings/double bonds [41]. The graphical representation of the reaction mechanism illustrated in the Fig. 6a.

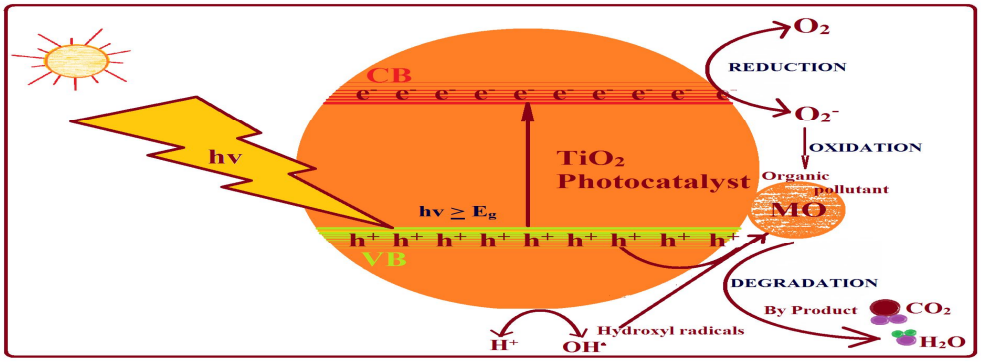

Fig. 6a: Photocatalytic degradation mechanism of Titanium Oxide nano photocatalyst with methyl orange dye under solar irradiation.

$TiO_2 + h\nu\ (<390\ nm) \rightarrow TiO_2\ (e_{CB}^- + h_{VB}^+)$
$TiO_2\ (e_{CB}^- + h_{VB}^+) \rightarrow TiO_2 + heat$
$TiO_2\ (e_{CB}^-) + O_2 \rightarrow TiO_2 + O_2^{\cdot -}$
$TiO_2\ (h_{VB}^+) + H_2O_{(ads)} \rightarrow TiO_2 + H^+ + OH^{\cdot}_{(ads)}$
$TiO_2\ (h_{VB}^+) + OH^- \rightarrow TiO_2 + OH^{\cdot}_{(ads)}$
$TiO_2\ (h_{VB}^+) + OM \rightarrow$ intermediates $TiO_2 + OM^{\cdot +}$
$OM + OH^{\cdot}_{(ads)} \rightarrow CO_2 + H_2O +$ salts

The resulting OH radical, being a very strong oxidizing agent can oxidize most of the organic dye and the mineral end-products not reactive towards hydroxyl radicals are degraded by nano TiO_2 photocatalysis with a decay rate of highly influenced by the semiconductor valance band edge position [41].

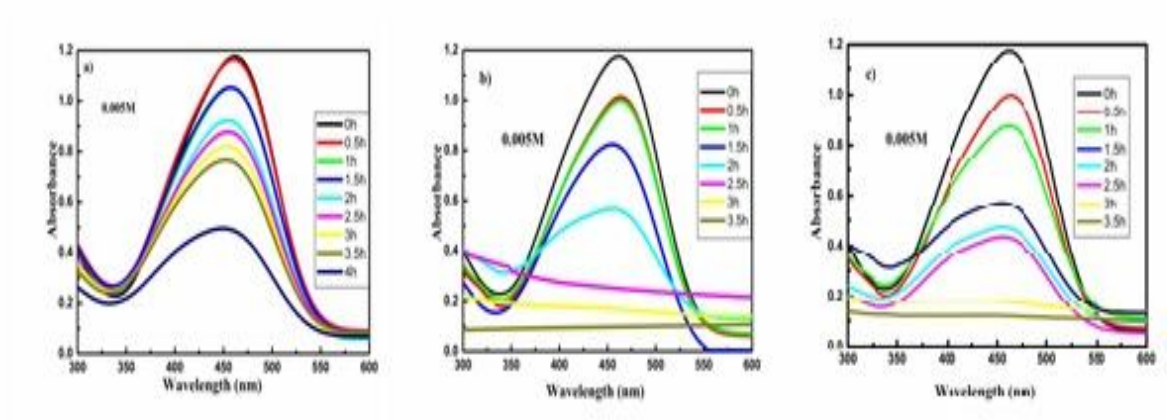

Fig. 6b: Photocatalytic degradation of methyl orange dye in the presence of as prepared b) calcined at 400°C and calcined at 600°C.

The organic dye is adsorbed on the surface of synthesized nanosized TiO2 particles, and then the photocatalytic decomposition takes place under visible light irradiation. Fig. 6b shows a strong UV absorption band at 466 nm, due to the presence of methyl orange. As the exposing time increases the absorption band completely disappears due to the photocatalytic property of the prepared TiO2 nanopowder samples. Degradation of dye is due to the increases of oxygen absorption site on the surface of TiO2 makes the H+ hydroxylation to form –Ti(OH)-O-Ti(OH)-, which improved the photogenerated holes H+ to change into OH free radical.

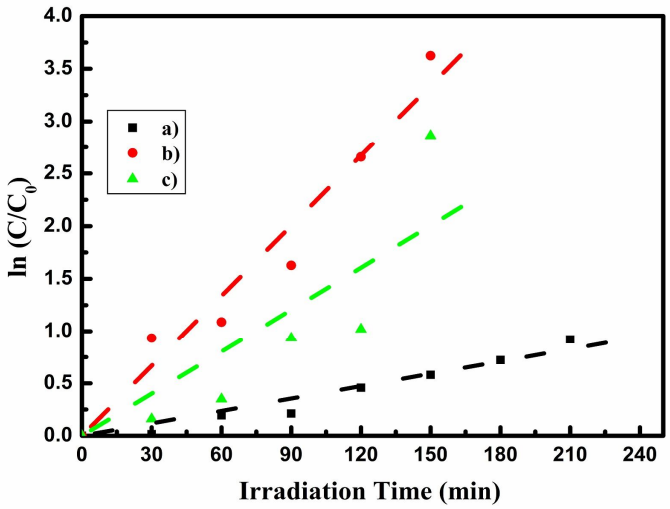

Fig. 6c: The $-\ln(C/C_o)$ Vs time plot for methyl orange by a) as synthesized b) anatase TiO_2 calcined at 400°C and c) at 600°C for 2h.

The photocatalytic decomposition of methyl orange organic pollutants on the surface of TiO_2 nanoparticles follows a pseudo-first-order kinetic law [44]. The relationships between $-\ln(C/C_o)$ and reaction time exists linear as shown in Fig. 6c. Values of apparent degradation rate constant k, could be estimated through linear regression analysis and reported in Table 2 as k= 0.00394 min^{-1}, k= 0.02227min^{-1} and k=0.01337min^{-1} for as prepared and calcined at 400 ^oC and 600 ^oC respectively. The residual concentration ratios C/C_o of MO versus degradation time is shown in Fig. 6d. It could be seen that TiO_2 400 showed higher photocatalytic activity than the others.

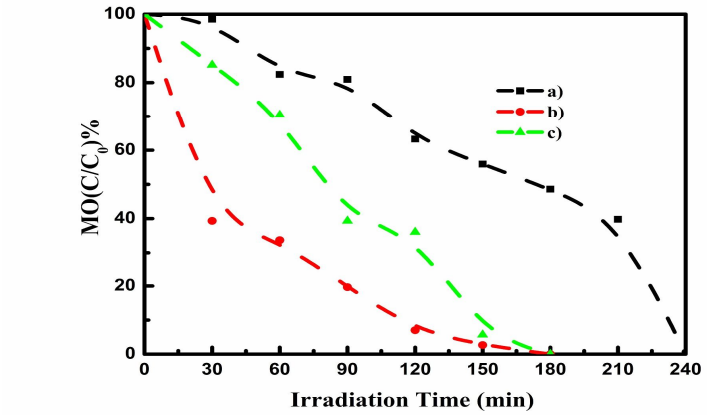

Fig. 6d: Degradation percentage of MO dye TiO_2 nano photocatalyst under visible light irradiation a) as prepared b) calcined at 400^oC and c) calcined at 600^oC for 2h.

The efficiency of the catalysts was found to follow the order: TiO2 400 > TiO2 600 > TiO2. The absorption spectra were recorded and rate of de-colourization was observed in terms of change in intensity at λmax of the methyl orange dye. The degradation percentage for dye was increased with time of illumination according to the equation Deg % = {(Ao-At)/(Ao-A∞) }*100% ,At → Absorbance after time t, A0 → Absorbance of dye at t=0 and Aα → Absorbance at t=4 h. The degradation percentage for dye was calculated and tabulated in Table 2. The decrease of dye degradation as a result that the generation of OH radicals on the catalyst surface is reduced since the active sites is covered by dye ions [43].

From Fig. 6e, exactly 100 % degradation of dye solution was obtained at 3.5h itself with the presence of anatase TiO_2 nano photocatalyst calcined at 400 ^oC having smallest crystallite size 9.8 nm and larger surface area. This indicates that the particle size has a major effect on the photocatalytic degradation. Visual change in the colour of the solution on irradiation also confirmed the photocatalytic activity of TiO_2 (Fig. 6f).

Fig. 6f: Visual change in the colour of methyl orange dye on irradiation with nano titanium oxide photocatalyst calcined at 400 ^oC.

Table 2: Photo catalytic degradation parameters for MO in the presence of anatase TiO_2 nanophotocatalyst

Sample detail	Degradation % at 3.5 h	Rate constant
As prepared	40	0.00394
TiO_2 400	100	0.02227
TiO_2 600	98	0.01337

IV. CONCLUSION

In this work, three samples of TiO_2 at various calcination temperatures were prepared by sol-gel method. Studies have been carried out for the identification of crystallinity, phase and particle size of prepared TiO_2 powder samples. With increasing heat treatment temperature, TiO_2 transforms from amorphous to anatase at 400°C and 600°C, accompanied by increase in crystal grain size. The results obtained from XRD and IR investigations facilitate assigning the obtained product to anatase structure. TEM measurements were used to examine the nano size crystallite/particles and the spherical morphology of samples. UV– Visible measurement showed that the onset of absorption was around 400 nm and the band gap varies from 3.24 to 3.06 eV with particle size. Effect of particle size and calcination temperature of the synthesized anatase TiO_2 on photocatalytic degradation of methyl orange under solar irradiation was verified. The anatase TiO_2 calcined at 400^oC shows better degradation because of its smaller particle size.

REFERENCES

[1] S. A. Parsons, and M. Williams, “Introduction in Advanced Oxidation Processes for Water and Wastewater Treatment”, S. A. Parsons ed, 1- 6, IWA Publishing, London, UK (2004).
[2] M. Zubair Alam, S. Ahmad, A. Malik, and M. Ahmad, Ecotoxicology and Environmental Safety, 73 (7)1620 (2010).
[3] C. O'neill, A. Lopez, S. Esteves, F. R. Hawkes, D. L. Hawkes, and S. J. Wilcox, Appl. Microbiol. Biotechnol., 53 (2) 249 (2000).
[4] L. Andronic, A. Enesca, C. Vladuta, and A. Duta, Chem. Engineer. J., 152 64 (2009).
[5] A. Fujishima, X. Zhang, and D. A. Tryk, Surf. Sci. Reports., 63[12] 515 (2008).
[6] M. M. Mohamed, and M. M. Al-Esaimi, J. Molecular Catal A: Chemical., 255 53(2006).
[7] C. Chen, Z. Wang, S. Ruan, B. Zou, M. Zhao, and F. Wu, Dyes Pigments., 77[1] 204 (2008).
[8] Z. M. El-Bahy, A. A. Ismail, and R. M. Mohamed, J. Hazardous Mater., 166 [1]138 (2009).
[9] M. Kanna, and S. Wongnawa, Mater. Chem. Phys., 110 166 (2008).
[10] A. Hosseinnia, M. K. Rad, and M. Pazouki, World Appl. Sci. J., 8 1327 (2010).
[11] K. Bubacz, J. Choina, D. Dolat, and A. W. Morawski, Polish. J. Environ. Stud., 19[4] 685 (2010).
[12] U. Diebold, Surf. Sci. Rep., 48 53 (2003).
[13] Y. B. Xie, and X. Z. Li, Mat. Chem. Phys., 95[1] 39 (2006).
[14] K. Tennakone, and K. G. U. Wijayantha, Appl. Catal. B: Environ, 57 9 (2004).
[15] P. Loebl, M. Huppertz, and D. Mergel, Thin Solid Films., 251 [1] 72 (1994).
[16] M. Wu, G. Lin, G. Wang, D. He, S. Feng, and R. Xu, Chem. Mater., 14 1974 (2002).
[17] P. D. Cozzoli, A. Kornowski, and H. Weller, J. Am. Chem. Soc., 125 (47) 14539 (2003).
[18] C. S. Kim, B. K. Moon, J. H. Park, B. C. Choi, and H. J. Seo, J. Cryst. Growth, 257 309(2003).
[19] K. Wilke, and H. D. Breuer, J. Photochem. Photobiol. A Chem., 121 49 (1999).
[20] M. S. P. Francisco, and V. R. Mastelaro, Chem. Mater., 14 2514 (2002).
[21] K. L. FrindellL, M. H. Bartl, A. Popitsch, and G. D. Stucky, Angew. Chem. Int. Ed., 41 959 (2002).
[22] S. Sakka, Am. Ceram. Soc. Bull., 64 1463 (1985).
[23] H. Kumazawa, H. Otsuki, and E. Sada, J. Mater. Sci. Lett., 12 839 (1993).
[24] D. C. Hague, and M. J. Mayo, J. Am. Ceram. Soc., 77 [7]1957 (1994).
[25] K. N. P. Kumar, K. Keizer, A. Burggraaf, T. Okubo, H. Nagamoto, and S. Morooka, Nature., 358 48 (1992).
[26] K. N. P. Kumar, J. Kumar, and K. Keizer, J. Am. Ceram. Soc., 77[5] 1396 (1994).
[27] Lisa M. Daniel, Ray L. Frost, and H. Y. Zhu, J. Colloid and Interface Sci., 316 72 (2007).
[28] D. Aphairaj, T. Wirumongkol, S. Pavasupree, and P. Limsuwan, Energy Procedia., 9 539 (2011).
[29] J. I. Langford, and A. J. C. Wilson, J. Appl. Crystallogr, 11 102 (1978).
[30] G. K. Williamson, and W. H. Hall, Acta Metall. Mater., 1 22-31 (1953).
[31] P. Scardi, M. Leoni, and R. Delhez, J. Appl. Crystallogr., 37 [3] 381 (2004).
[32] M. Razavi, M. R. Rahimipour, and A. H. Rajabi Zamani, J. Alloys. Compd., 436 142 (2007).
[33] M. Razavi, M. R. Rahimipour, and R. Mansoori, J. Alloys. Compd., 450 463 (2008).
[34] G. Carja, and G. Delahay, Appl. Catal. B.Environmental, 47[1] 59 (2004).

[35] J. Yang, H. Bai, X. Tan and J. Lian, Appl Surf. Sci., 253 1988 (2006).

[36] C. Wen, H. Ssu, T. Jeou, C. Hsin, and H. Tzu, J. Chemosphere., 66 2142 (2007).
[37] G. Socrates, "Infrared and Raman Characteristic Group Frequencies: Tables and Charts," 3rd ed, John Wiley & Sons Ltd, England (2001).
[38] S. Sakthivel, M. V. Shankar, M. Palanichami, B. Arabindoo, D. W. Bahnemann, and V. Murugesan, Water Res., 38 [13] 3001(2004).
[39] Y. Wang, and N. Herron, J. Phys. Chem., 95 525-532 (1991).
[40] M. A. Rauf and S. S. Ashraf, "In: A. R. Lang, Ed., Dyes and Pigments": New Research Nova Science Publishers Inc Hauppauge (2009).
[41] M. R. Hoffmann, S.T. Martin, W. Choi, and D.W. Bahnemann, Chem. Rev., 95 69 (1995).
[42] S. B. Sakthivela, M. V. Neppolian, B. Shankar, M. Arabindoo, V. Palanichamy, and V. Murugesan, Sol. Energy Mater. Sol. Cells., 77 65 (2003).
[43] I. Poulios, and I. Tsachpinis, J. Chem. Technol. Biotechnol., 74 349 (1999).

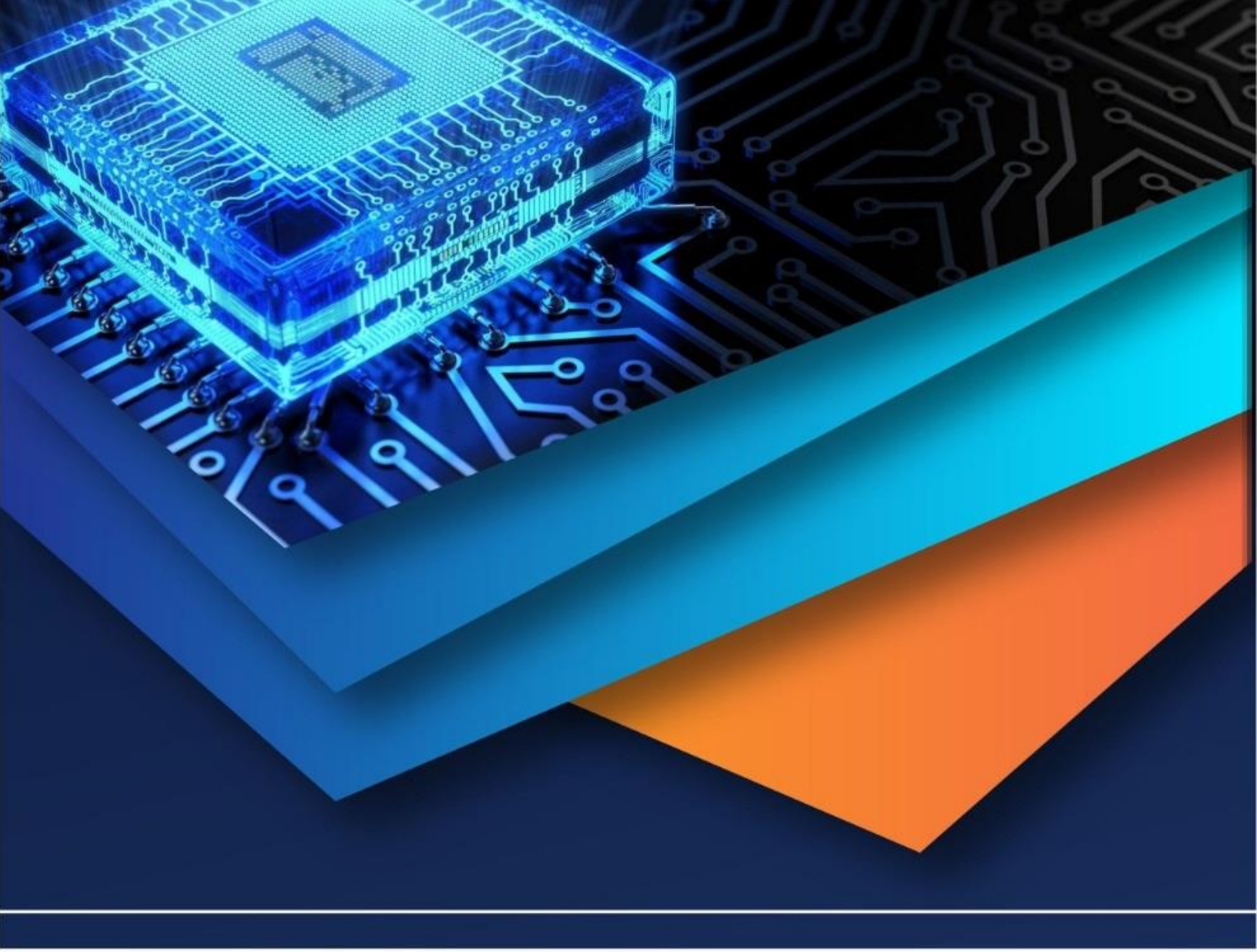

10.22214/IJRASET

45.98

IMPACT FACTOR: 7.129

IMPACT FACTOR: 7.429

INTERNATIONAL JOURNAL FOR RESEARCH

IN APPLIED SCIENCE & ENGINEERING TECHNOLOGY